BRAIN RESEARCH 1388 (2011) 167–177

available at www.sciencedirect.com

ScienceDirect

www.elsevier.com/locate/brainres

BRAIN RESEARCH

Research Report

Altered gray matter morphometry and resting-state functional and structural connectivity in social anxiety disorder☆

Wei Liao[a,1], Qiang Xu[a,1], Dante Mantini[b], Jurong Ding[a], João Paulo Machado-de-Sousa[c], Jaime E.C. Hallak[c], Clarissa Trzesniak[c], Changjian Qiu[d], Ling Zeng[a], Wei Zhang[d,**], José Alexandre S. Crippa[c], Qiyong Gong[e], Huafu Chen[a,*]

[a]Key Laboratory for NeuroInformation of Ministry of Education, School of Life Science and Technology, University of Electronic Science and Technology of China, Chengdu 610054, PR China
[b]Laboratory of Neuro-psychophysiology, K. U. Leuven Medical School, Leuven, Belgium
[c]Department of Neuroscience and Behavior, Ribeirão Preto Medical School, University of São Paulo and National Institute for Translational Medicine (INCT-TM, CNPq), São Paulo, Brazil
[d]Mental Health Center, Department of Radiology, West China Hospital of Sichuan University, Chengdu 610041, PR China
[e]Huaxi MR Research Center (HMRRC), Department of Radiology, West China Hospital of Sichuan University, Chengdu 610041, PR China

ARTICLE INFO

Article history:
Accepted 7 March 2011
Available online 12 March 2011

Keywords:
Social anxiety disorder
Gray matter morphometry
Resting state
Functional connectivity
Structural connectivity

ABSTRACT

In social anxiety disorder (SAD), impairments in limbic/paralimbic structures are associated with emotional dysregulation and inhibition of the medial prefrontal cortex (MPFC). Little is known, however, about alterations in limbic and frontal regions associated with the integrated morphometric, functional, and structural architecture of SAD. Whether altered gray matter volume is associated with altered functional and structural connectivity in SAD. Three techniques were used with 18 SAD patients and 18 healthy controls: voxel-based morphometry; resting-state functional connectivity analysis; and diffusion tensor imaging tractography. SAD patients exhibited significantly decreased gray matter volumes in the right posterior inferior temporal gyrus (ITG) and right parahippocampal/hippocampal gyrus (PHG/HIP). Gray matter volumes in these two regions negatively correlated with the fear factor of the Liebowitz Social Anxiety Scale. In addition, we found increased functional connectivity in SAD patients between the right posterior ITG and the left inferior occipital gyrus, and between the right PHF/HIP and left middle temporal gyrus. SAD patients had increased right MPFC volume, along with enhanced structural connectivity in the genu of the corpus callosum. Reduced limbic/paralimbic volume, together with increased resting-state functional connectivity, suggests the existence of a compensatory mechanism in SAD. Increased MPFC volume, consonant with enhanced structural connectivity, suggests a long-time overgeneralization of structural connectivity and a role of this area in the mediation of clinical severity. Overall, our

☆ The authors declare no competing interests.

* *Correspondence to:* H. Chen, Key Laboratory for NeuroInformation of Ministry of Education, School of Life Science and Technology, University of Electronic Science and Technology of China, Chengdu 610054, PR China. Fax: +86 28 83208238.
** *Correspondence to:* W. Zhang, Mental Health Center, West China Hospital of Sichuan University, Chengdu 610041, PR China. Fax: +86 28 85582944.
E-mail addresses: chenhf@uestc.edu.cn (H. Chen), Weizhang27@163.com (W. Zhang).
[1] These authors contributed equally to this work.

doi:10.1016/j.brainres.2011.03.018

results may provide a valuable basis for future studies combining morphometric, functional and anatomical data in the search for a comprehensive understanding of the neural circuitry underlying SAD.

1. Introduction

Social anxiety disorder (SAD) generally refers to the excessive fear and avoidance of a wide array of social situations (Filho et al., 2010; Stein and Stein, 2008). There is increasing evidence that altered brain functional patterns underlie the processing of emotional stimuli under conditions of social fear and anxiety (Etkin and Wager, 2007; Freitas-Ferrari et al., 2010; Phan et al., 2006; Stein et al., 2002; Straube et al., 2004; Tillfors et al., 2001). Specifically, the most consistent findings from functional neuroimaging studies in SAD patients indicate increased activity in the limbic/paralimbic system (amygdala, insula, parahippocampus and hippocampus, and dorsal anterior cingulate cortex) and altered activity in the prefrontal cortex (Blair et al., 2008a,b; Gentili et al., 2008; Lorberbaum et al., 2004; Stein et al., 2002; Straube et al., 2004). In addition, there is significant and consistent evidence of hyperactivation of limbic/paralimbic structures associated with emotional dysregulation during the processing of facial emotion and in classical exposure situations (Mathew et al., 2001; Phan et al., 2006; Stein et al., 2002). Furthermore, the medial prefrontal cortex (MPFC) plays a pivotal role in the modulation and inhibition of excessive limbic activity (Etkin et al., 2006; Tillfors et al., 2001, 2002). This is a strong indication that anxiety might be associated with an imbalance in limbic-cortical connectivity (Bishop, 2007; Warwick et al., 2008). Together, these results suggest that brain functional changes in SAD involve impaired long-range communication during sensory and emotional processing (Danti et al., 2010) and at rest (Liao et al., 2010b).

Brain morphometry analysis is complementary to functional investigations, as it is a powerful tool to detect brain abnormalities that may vary progressively during the course of illness (Ferrari et al., 2008). Potts and colleagues found no significant differences between the volumes of the caudate, putamen, thalamus, and whole brain of SAD patients and healthy controls (Potts et al., 1994). More recently, Irle and coworkers found that generalized SAD patients had reduced amygdalar and hippocampal size (Irle et al., 2010). It is worth noting that both studies used a region of interest (ROI) to investigate brain morphometry. This may potentially bias the detection of positive findings (Ferrari et al., 2008; Freitas-Ferrari et al., 2010). More importantly, this approach is not adequate for the study of large neural systems. Accordingly, it is still unclear whether gray matter volume alterations in SAD are related to altered functional connectivity within brain networks.

The analysis of task-independent, resting-state functional connectivity may allow for a better understanding of SAD mechanisms (Warwick et al., 2008). One pioneering resting-state functional magnetic resonance imaging (fMRI) study on generalized anxiety disorder (GAD) has demonstrated that aberrant brain networks selectively interact with the basolateral and centromedial subregions of the amygdala (Etkin et al., 2009). More recently, our group found diffuse changes on widely distributed brain networks in SAD patients at rest (Liao et al., 2010a). However, functional connectivity analysis is based on low-frequency spontaneous fluctuations of the blood oxygen level-dependent (BOLD) signal between distant brain regions. It is, therefore, unable to reveal whether they are anatomically connected or not (Honey et al., 2009). Conversely, diffusion tensor imaging (DTI) fiber tractography allows the study of human structural connectivity (Catani et al., 2002; Johansen-Berg and Rushworth, 2009). Recently, a DTI study on SAD documented reduced fractional anisotropy (FA) in the right uncinate fasciculus, underlying aberrant limbic-prefrontal interactions (Phan et al., 2009). In addition, increased gray matter volume is likely to reflect exuberant synaptic connectivity (Supekar et al., 2010). These studies suggested the importance of studying changes in structural connectivity to improve the understanding of the neural underpinnings of SAD.

The main objective of this study was to test whether altered gray matter volume is associated with altered functional and structural connectivity in SAD. For the first time, three imaging modalities (voxel-based morphometry [VBM], resting-state functional connectivity, and DTI tractography) were combined in order to perform a comprehensive evaluation of the neural circuitry underlying SAD.

2. Results

2.1. *Clinical and demographic data*

The group's demographics and clinical scores are shown in Table 1. Compared with healthy controls (HC), SAD patients had significantly higher scores (total, fear factor, and avoidance factor) in the Liebowitz Social Anxiety Scale (LSAS), the Hamilton Anxiety Rating Scale (HAMA), and the Hamilton Depression Rating Scale (HAMD). They also had higher levels of anxiety as assessed with the Spielberger State-Trait Anxiety Inventory (STAI). The remaining characteristics did not differ across groups.

2.2. *Morphometry analysis*

Compared with HC, SAD patients had significantly decreased gray matter volumes in the right posterior inferior temporal gyrus (ITG), the parahippocampal gyrus (PHG), and the left hippocampal gyrus (HIP). Increased gray matter volume in SAD patients was found in the right MPFC (Fig. 1, Table S1). Significant negative correlations ($p<0.05$, Bonferroni corrected) were observed between the fear factor of the LSAS and gray matter volumes in the right posterior ITG ($r=-0.69$, $p=0.004$) and left PHG ($r=-0.69$, $p=0.004$) in the SAD group. There were no significant correlations in the HC group between gray matter volume in those brain regions and LSAS scores (Table S1).

Table 1 – Clinical and demographic data.

	SAD ($n=18$) [a]	HC ($n=18$)	SAD vs. HC	
			T value	p value
Gender (male/female)	12/6	13/5	–	0.73 [b]
Age (y)	22.67±3.77	21.89±3.69	0.63	0.54
Education (y)	14.11±1.53	14.17±2.04	–0.09	0.93
Duration (m)	49.22±40.17	–	–	–
LSAS				
Total score	54.39±11.96	19.11±7.89	10.45	<0.0001
Fear factor	28.50±6.20	8.50±5.07	10.59	<0.0001
Avoidance factor	25.89±7.32	10.61±4.86	7.38	<0.0001
HAMD	7.33±6.15	1.06±1.59	4.19	<0.001
HAMA	6.39±4.97	0.94±1.55	4.43	<0.0001
STAI				
STAI-T	48.33±7.40	32.67±4.97	7.46	<0.0001
STAI-S				
Pre-scan	41.11±8.66	31.28±4.75	4.22	<0.001
Post-scan	37.11±9.50	32.94±7.12	1.49	0.15
Head Motion				
Translation (mm)	0.03±0.01	0.04±0.02	–0.61	0.55
Rotation (°)	0.03±0.01	0.03±0.02	–0.20	0.84

Abbreviations: SAD=social anxiety disorder; HC=healthy controls; LSAS=Liebowitz Social Anxiety Scale; HAMA=Hamilton Anxiety Rating Scale; HAMD=Hamilton Depression Rating Scale; STAI=Spielberger State-Trait Anxiety Inventory.

[a] Questionnaire data are given as means±standard deviation (SD).

[b] p Value was obtained by the Kruskal–Wallis test. Other p values were obtained by two-sample, two-tailed t-tests.

2.3. *Functional connectivity analysis*

The right posterior ITG was found to be functionally connected in both groups with the bilateral dorsolateral prefrontal, the posterior parietal, and the middle temporal cortex; negative correlations mainly involving the inferior and middle occipital cortices, and the bilateral precentral gyrus (Fig. 2A). Compared with HC, SAD patients had increased functional connectivity (weak negative connection) in the left inferior occipital gyrus (IOG) (Fig. 3A). Significant positive correlations ($p<0.05$, Bonferroni corrected) were observed between the degree of functional connectivity in the left IOG and the total ($r=0.58$, $p=0.012$) and avoidance ($r=0.60$, $p=0.008$) scores in the LSAS (Fig. 3A and Table S2).

The left PHG was functionally connected with the bilateral anterior superior temporal gyrus, the hippocampal gyrus, and the entorhinal cortex (Kahn et al., 2008) in both groups. Significant negative connectivities included mainly a right fronto-parietal network (Fig. 2B). Compared with HC, SAD patients had increased functional connectivity in the left middle temporal gyrus (MTG) (Fig. 3B). We observed positive correlations ($p<0.05$, uncorrected) between the fear factor of the LSAS ($r=0.54$, $p=0.039$) and the degree of functional connectivity in the left MTG for the SAD group. This analogous correlation was not significant in the HC group ($r=-0.19$, $p=0.456$) (Table S2).

The right MPFC showed significantly positive functional connectivity in the posterior cingulate cortex/precuneus, the bilateral inferior parietal, gyrus, middle temporal, and superior frontal gyrus. These regions are considered to be part of the default mode network (DMN) (Raichle et al., 2001). Both groups had significantly negative functional connectivity regions involving executive control network (ECN) and the dorsal attention network (DAN) (Corbetta and Shulman, 2002) (Fig. 2C). There were no significant differences in functional connectivity between SAD patients and HC when the right MPFC was used as seed.

2.4. *Structural connectivity analysis*

Structural connections of the right posterior ITG included the arcuate fasciculus fiber bundle (Fig. 4A). This is a lateral associative bundle composed of long and short fibers connecting the perisylvian cortex with the frontal, parietal, and temporal lobes. A seed ROI located in the left PHG showed the inferior fronto-occipital fasciculus, a ventral associative bundle arising from the ventral occipital lobe and going toward the orbitofrontal cortex (Fig. 4B). When the seed ROI was located in the right MPFC, fiber tracts passed through the genu (anterior portion) of the corpus callosum to interconnect left and right prefrontal cortical regions (Fig. 4C). Comparing SAD patients and HC, the fiber density (weight) and mean FA showed significant increase ($p<0.05$, Bonferroni corrected) only in fibers passing through the genu of the corpus callosum. In addition, both the fiber density and mean FA of the three seed ROI showed no significant correlations with the LSAS.

3. Discussion

To the best of our knowledge, the present cross-sectional study is the first to combine structural MRI, resting-state functional connectivity, and diffusion tensor imaging tractography to investigate alterations in limbic and frontal regions in SAD. Patients had significantly decreased gray matter volumes in the right ITG and right limbic/paralimbic structures (PHG and HIP) that are compatible with increased functional connectivity. In addition, increased gray matter volume was observed in the right MPFC, along with enhanced structural connectivity.

Only two earlier studies using brain morphometry analyses in SAD are available to date. The first indicated no difference in striatal structures (caudate, putamen, and thalamus) (Potts et al., 1994), while the second found reduced amygdalar and hippocampal volumes (Irle et al., 2010). Since these studies performed ROI-based morphometry comparisons, the possibility of both false positive and false-negative findings should be considered (Freitas-Ferrari et al., 2010). As opposed to those previous studies, we have now used an automated whole-brain VBM-based technique for the investigation of SAD, which allows assessing areas not previously investigated by the ROI-based method. Decreased right posterior ITG volume was found in SAD patients compared to HC. Functionally, the ITG is involved in visual perception (Ishai et al., 1999) and is linked to the ventral visual pathway (Baddeley et al., 1997). Furthermore, the ITG has reciprocal connections with the amygdala and the orbitofrontal cortex, which are predominantly involved in the affective processing of negative expressions (Iidaka et al., 2001). It has also been reported that the processing of external social cues in social phobia is characterized by a negative bias (Arrais et al., 2010; Clark and Wells, 1995; Machado-de-Sousa et al., 2010).

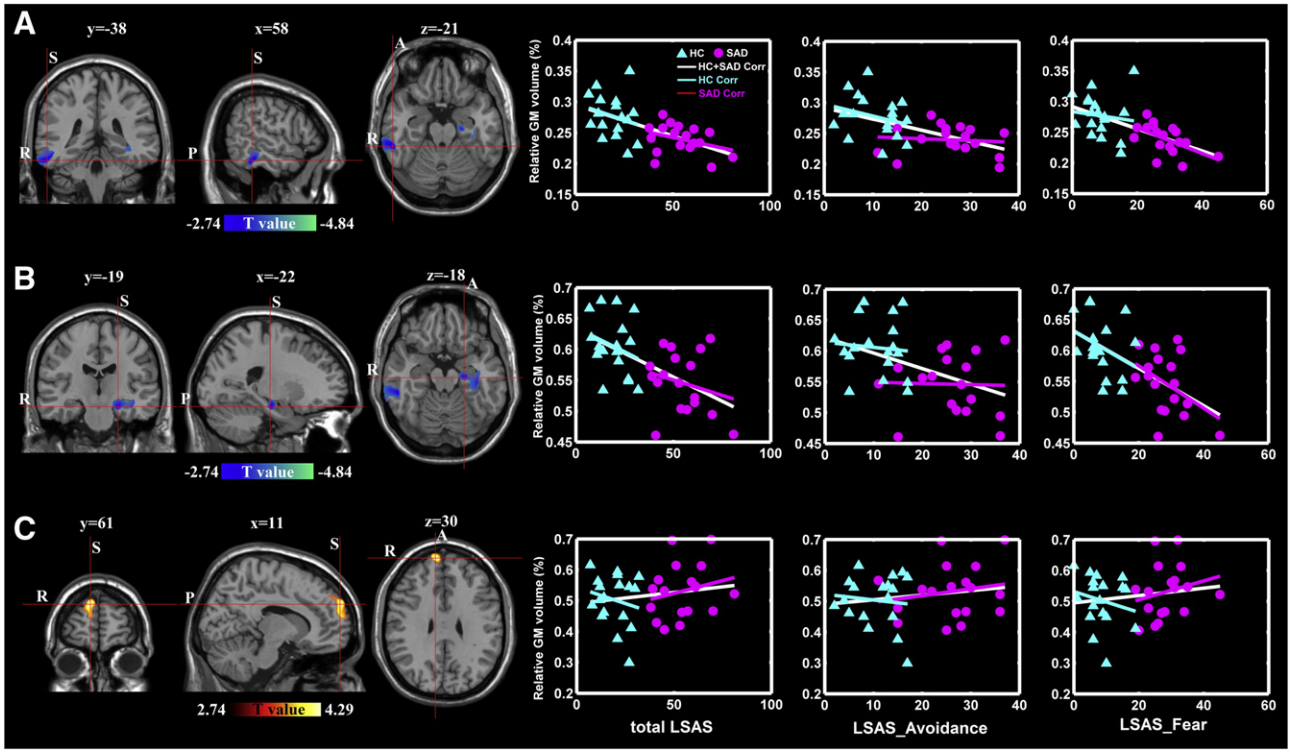

Fig. 1 – Statistical parametric maps of voxel-based morphometry analysis comparing SAD patients and HC and correlations between gray matter volume and the LSAS. (A). Decreased gray matter volume in the right posterior ITG; (B). Decreased gray matter volume in the left PHG; (C). Increased gray matter volume in the right MPFC. Hot and cold colors indicate brain regions with significantly increased and decreased gray matter volumes between SAD patients and HC. The color scale represents *T* values using two-sample t-tests ($p < 0.05$, AlphaSim corrected). Correlations between gray matter volume in these three regions and the LSAS (including total score, fear factor, and avoidance factor) are displayed on the right side. The details of statistically significant correlations are listed in Table S1.

Additionally, the gray matter volume in the right ITG negatively correlated with the fear factor of the LSAS in SAD patients, but not in HC. This association points to a possible anatomical substrate of SAD expressed by volumetric abnormalities.

We also calculated resting-state functional connectivity maps, using the right ITG as a seed ROI. This analysis can assess differences in the crosstalk among brain regions, reflecting abnormal activations in response to given tasks. Functional connectivity investigations have shown that resting-state brain activity is spatially organized in sets of specific coherent patterns that putatively correspond to a specific brain functions (Cole et al., 2010). Our results showed a lateral fronto-parietal ECN (Koechlin and Summerfield, 2007; Seeley et al., 2007; Vincent et al., 2008) that is involved in the cognitive control of both emotional and non-emotional material (Duncan and Owen, 2000; Miller and Cohen, 2001; Ochsner and Gross, 2005). It has been previously hypothesized that amygdalo-fronto-parietal coupling in GAD patients reflects the "habitual engagement of a cognitive control system to regulate excessive anxiety" (Etkin et al., 2009).

We also found increased functional connectivity (weak negative connection) in the left IOG. A previous emotion-based fMRI study documented that the visual cortex is activated during exposure to ocial threat in SAD (Goldin et al., 2009b). Moreover, social anxiety-related neural responses were different prior to and after treatment (Kilts et al., 2006). The significant positive correlations between the total LSAS scores, the scores in the avoidance factor of the LSAS, and the degree of functional connectivity in the left IOG provide further evidence for an abnormal processing of visual information in SAD.

The PHG and HIP are thought to play a key role in mediating fear and anxiety, consistent with our observation of reduced volumes in these limbic/paralimbic structures in SAD patients. Our finding is in agreement with a previous study in which SAD patients had significantly reduced hippocampal size (Irle et al., 2010). This has also been reported to occur in other anxiety disorders such as post-traumatic stress disorder (Wignall et al., 2004), obsessive–compulsive disorder (Atmaca et al., 2008), and panic disorder (Massana et al., 2003). Furthermore, various functional neuroimaging studies have provided significant and consistent evidence of abnormal brain functioning in SAD, mostly related to limbic structures (Goldin et al., 2009b; Kilts et al., 2006; Stein et al., 2002; Straube et al., 2004). For instance, the processing of facial expressions in SAD patients was associated with increased activation or exaggerated responses in the PHG and HIP for angry faces versus neutral ones (Stein et al., 2002; Straube et al., 2004). Further studies on facial emotion processing in SAD have provided additional support for this hypothesis (Birbaumer et al., 1998; Schneider et al., 1999; Tillfors et al., 2001). In our study, gray matter volume negatively

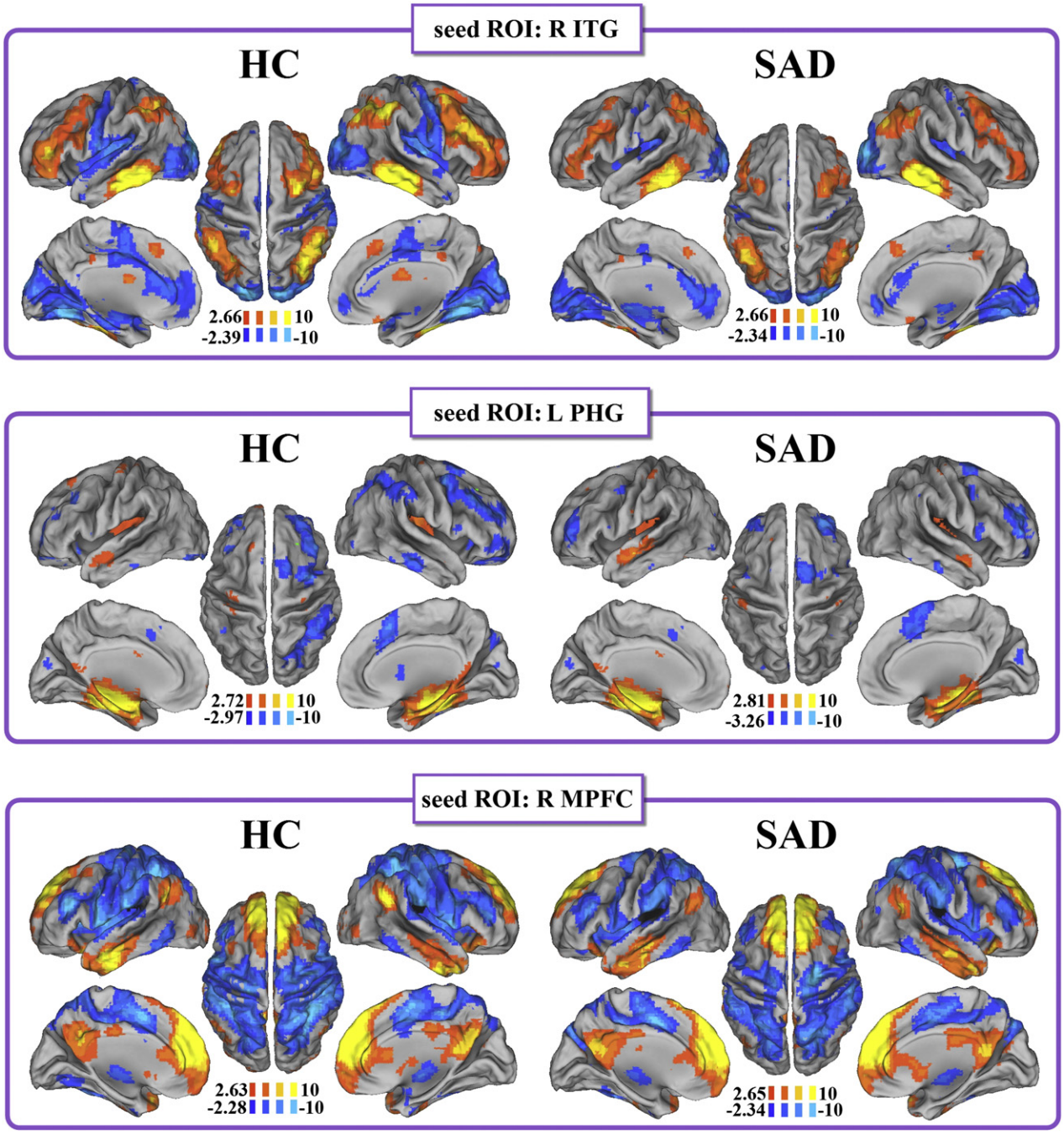

Fig. 2 – Resting-state functional connectivity maps for HC (left column) and SAD patients (right column). Seed ROI (regions with gray matter volume reduction) located in the right posterior ITG (MNI coordinates: 58, –38, –21) (top row). Seed ROI (regions with gray matter volume reduction) located in the left PHG (MNI coordinates: –22, –19, –18) (middle row). Seed ROI (regions with gray matter volume increase) located in the right MPFC (MNI coordinates: 11, 61, 30) (bottom row). Hot and cold colors indicate brain regions with significant positive and negative temporal correlations with the selected seed ROI, respectively. Color scales represent *T* values in each functional connectivity map using one-sample *t*-test ($p < 0.05$, false discovery rate criterion for multiple comparisons).

correlated with the fear factor of the LSAS in the SAD group only. Thus, we would argue that sustained emotional dysregulation could lead to progressive atrophy of the PHG and HIP responsible for emotional processing and social behaviors.

The functional connectivity analysis involving the right PHG/HIP as seed showed increased functional connectivity in the right MTG in SAD patients compared to controls. Previous studies observed increased neural activity related to different

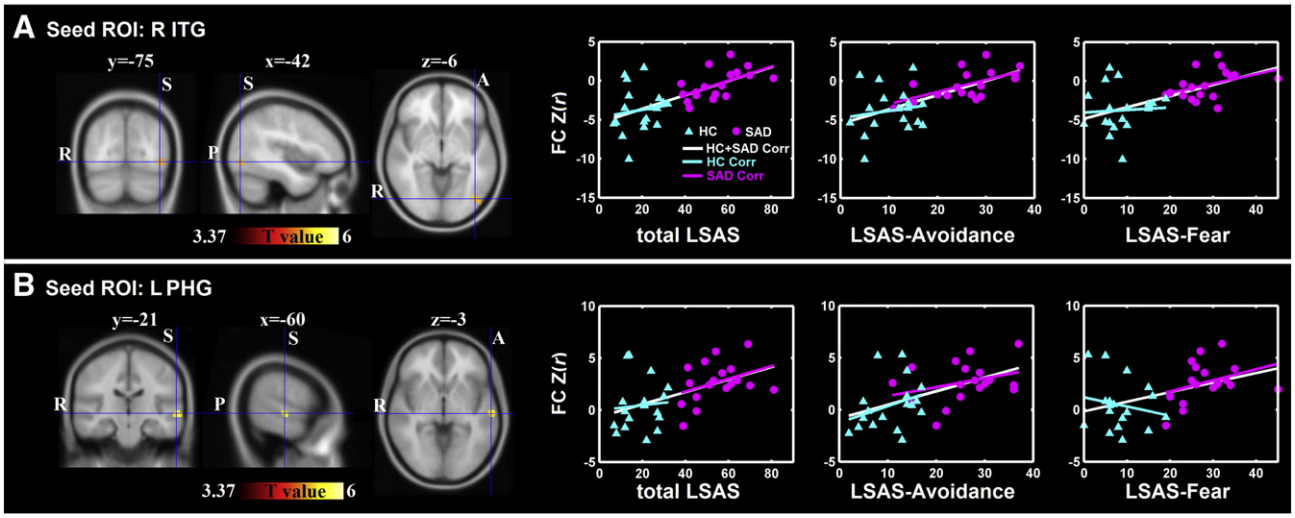

Fig. 3 – Increased resting-state functional connectivity in SAD patients compared to HC. (A). Regions of increased resting-state functional connectivity in the left inferior occipital gyrus (MNI coordinates: –42, –75, –6; Brodmann's area 19; voxel size = 22 mm^3) with the seed ROI located in the right posterior ITG; (B). Regions showing increased resting-state functional connectivity in the left middle temporal gyrus (MNI coordinates: 60, –21, –3; Brodmann's area 21; voxel size = 25 mm^3) with the seed ROI located in the left PHG. Hot colors indicate brain regions with significantly increased functional connectivity. The color scale represents *T* values using two-sample *t*-tests ($p < 0.05$, AlphaSim corrected). Correlations between the degree of functional connectivity (*Z*(*r*) value) of these two regions and the LSAS (including total score, fear factor, and avoidance factor, respectively) are displayed on the right side. The details of statistically significant correlations are listed in Table S2.

facial emotional expressions in subjects with SAD not only in the amygdala and the insula, but also in medial temporal structures (Gentili et al., 2008; Stein et al., 2002). For instance, SAD patients had increased parahippocampal–hippocampal activity and anxiety symptoms during a stressful public speaking task, which was reversed after treatment with the SSRI citalopram (Furmark et al., 2005). We therefore speculate that increased connectivity in the right MTG network is effective in the inhibition or extinction of excessive cortico-limbic activity in anxiety disorders in general, and in SAD in particular.

Another finding was the presence of significantly increased right MPFC volume. The MPFC, an important brain region in the neurocircuitry of SAD, plays a pivotal role in the modulation of

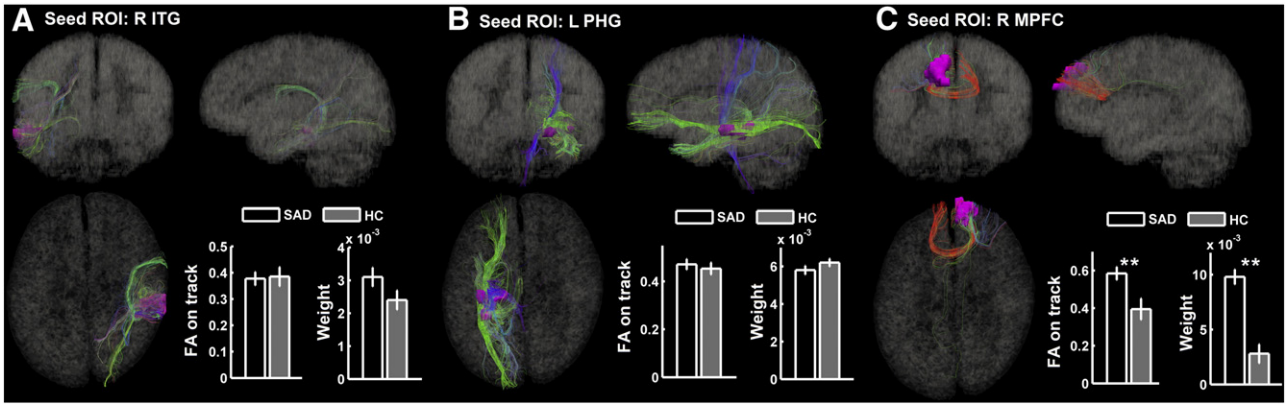

Fig. 4 – Fiber tracts of three selected ROI (one subject from the HC group for display purposes). (A). Fiber tracts in the arcuate fasciculus passing through the right posterior ITG; (B). Fiber tracts in inferior fronto-occipital fasciculus passing through the left PHG; (C). Fiber tracts in the genu (anterior portion) of the corpus callosum passing through the right MPFC. The color-coding of the obtained fibers is based on the standard RGB code applied to the vector at every segment of each fiber (red: medio-lateral plane, green: dorsoventral orientation, blue: rostro-caudal direction). Bars represent mean values of fiber density and mean FA on track. Vertical bars indicate estimated standard errors. ** represents the statistical significance with $p < 0.05$, Bonferroni corrected.

excessive limbic activity (Etkin et al., 2006; Tillfors et al., 2001, 2002; Warwick et al., 2008). For example, in two positron emission tomography studies on SAD, Tillfors and colleagues suggested that regional cerebral blood flow (rCBF) reductions in the frontal cortex is associated with increased rCBF in the amygdala, HIP, and ITG, all of which have been implicated in emotional dysregulation and failure to inhibit negative affect (Tillfors et al., 2001, 2002). In an fMRI study, Etkin and coworkers revealed that increased activity in the ventromedial prefrontal cortex and decreased activity in the amygdala were involved in the extinction of conditioned fear (Etkin et al., 2006). In a resting-state single photon emission computed tomography study, Warwick and colleagues demonstrated increased rCBF in the frontal cortex of SAD patients (Warwick et al., 2008). Although decreases in activity are not necessarily related to decreases in volume (Ferrari et al., 2008), we argue that an increased right MPFC volume may contribute to the progressive and sustained modulation and inhibition of excessive limbic activity.

The MPFC is thought to provide information from prior experiences in the form of memories during the construction of self-relevant mental simulation (Buckner et al., 2008). Although aberrant global coherent connectivity in the MPFC of SAD patients has been observed at rest (Liao et al., 2010a) and during listening to threat-related words (Zhao et al., 2007), we found no significant differences in functional connectivity within this brain region. One possible reason is that volume increases are not necessarily related to increases in functional connectivity.

Another remarkable finding was that the fiber density (weight) and mean FA on track were significantly increased in the genu of the corpus callosum when the seed ROI was located in the right MPFC for the structural connectivity analysis. The genu of the corpus callosum was found to connect the left and right prefrontal cortical regions. The activity in the dorsal anterior cingulate cortex (dACC) anterior to the genu of the corpus callosum has been consistently associated with mood states (Blair et al., 2008a; Critchley, 2003; Smith et al., 1999) and correlated with volume (Boes et al., 2008). This region is activated, among other situations, when subjects process harsh and disgusted facial expressions (Amir et al., 2005; Blair et al., 1999; Phan et al., 2006; Shin and Liberzon, 2010) or evaluate emotional information (Phan et al., 2003). Together, the dACC and the MPFC are thought to implement regulatory strategies and to direct attentional control, in addition to reducing cognitive conflict (Kerns et al., 2004). This neural circuitry would underlie emotional regulation problems in patients with SAD during cognitive reappraisal (Goldin et al., 2009a). The modulating function of the MPFC and the dACC seems not to be restricted to the processing of facial affect, but to also occur in intrinsic structural connectivity associated with long-time overgeneralization.

Some limitations of the study and future directions for research in the field deserve to be mentioned. First, further multimodal studies will be necessary to promote deeper insight into the neurophysiopathology of SAD. In addition, although we recruited a consistent number of SAD patients who were medication- and comorbidity-free, our findings should be extended to larger SAD samples in the future, especially for VBM analysis.

The present study used a multimodal neuroimaging approach comprising structural MRI, resting-state functional connectivity, and diffusion tensor imaging tractography to investigate the alterations of limbic and frontal areas in SAD. Reduced limbic/paralimbic gray matter volume, together with increased resting-state functional connectivity, suggests the existence of a compensatory mechanism in SAD. Increased MPFC gray matter volume, consonant with enhanced structural connectivity, suggests a long-time overgeneralization of structural connectivity and a role of this structure in mediating clinical severity. Overall, our results may provide a valuable basis for future studies combining morphometric, functional, and anatomical data for a comprehensive understanding of the neural circuitry underlying SAD.

4. Experimental procedures

4.1. *Participants*

The study was approved by the local ethics committee of Huaxi Hospital, Sichuan University, and written informed consent was obtained from all subjects.

The SAD group was composed of 18 patients (22.67 ± 3.77 years, all right-handed) recruited through the Mental Health Center of Huaxi Hospital, China (Table 1). Generalized SAD diagnosis was determined by consensus between two attending psychiatrists and a trained interviewer using the patient version of the Structured Clinical Interview for the DSM-IV (SCID). Subjects who presented other psychiatric disorders according to the SCID were excluded from the sample. Additionally, we excluded individuals in treatment with psychotropic medication or in use of psychoactive substances, those presenting neurological or general medical conditions or those who had received previous treatment for SAD (either pharmacological or psychotherapeutic).

The comparison group consisted of 18 age-, sex-, and education-matched HC (21.89 ± 3.69 years, all right-handed). The SCID was used to confirm the absence of past or current psychiatric or neurological illness. HC were medication-free at the time of the scanning. Additionally, they were interviewed to confirm that there was no history of psychiatric illness among their first-degree relatives. All participants in the two groups were evaluated with the LSAS, STAI, HAMA, and HAMD. More specifically, the STAI was administered in two parts: the STAI-State score, which measures the level of state anxiety at the time of completing the scale, and the STAI-Trait score, which measures the inherent trait anxiety level of the subject. The STAI-Trait was completed immediately before and after the MRI scanning (pre-scanning and post-scanning) session (Campbell et al., 2007).

4.2. *Data acquisition*

All subjects underwent structural, functional and DTI scanning using a 3.0T GE-Signa MRI scanner (EXCITE, General Electric, Milwaukee, USA) at Huaxi MR Research Center. Functional images were acquired using a single-shot, gradient-recalled echo planar imaging sequence (TR = 2000 ms, TE = 30 ms and flip angle = 90º, FOV = 24 cm, in-plane matrix = 64 × 64, voxel size = 3.75 × 3.75 × 5, without inter-slice gap, and 30 transverse slices). For each subject, a total of 205 volumes were acquired, resulting

in a total scan time of 410 s. Subjects were instructed simply to rest with their eyes closed, not to think of anything in particular, and not to fall asleep. Axial anatomical images were acquired using a volumetric three-dimensional spoiled gradient recalled (SPGR) sequence (TR = 8.5 ms, TE = 3.4 ms, flip angle = 12º, field of view = 240 × 240 mm^2, matrix size = 512 × 512, voxel size = 0.47 × 0.47 × 1 mm^3, and 156 axial slices). The DTI acquisition used a single-shot spin-echo planar imaging sequence in contiguous axial planes covering the whole brain (TR = 12000 ms, TE = 71.4 ms, field of view = 240 × 240 mm^2, flip angle = 90º, matrix size = 256 × 256, voxel size = 0.94 × 0.94 × 3 mm^3, 50 slices). At each slice position, except for S0 (b = 0 s/mm^2), a single b-value (b = 1000 s/mm^2) was applied to 15 non-collinear gradient directions.

4.3. *Voxel-based morphometry analysis*

Voxel-based morphometry analysis (Ashburner, 2009) was performed using SPM8 (http://www.fil.ion.ucl.ac.uk/spm). First, all T1-weighted anatomical images were manually reoriented to place the anterior commissure at the origin of the three-dimensional Montreal Neurological Institute (MNI) space. The images were then segmented into gray matter, white matter, and cerebrospinal fluid (CSF) (Ashburner and Friston, 2005). A diffeomorphic non-linear registration algorithm (diffeomorphic anatomical registration through exponentiated lie algebra—DARTEL) (Ashburner, 2007) was used to spatially normalize the segmented images. This procedure generated a template for a group of individuals. The resulting images were spatially normalized into the MNI space using affine spatial normalization. An additional processing step consisted of multiplying each spatially normalized gray matter image by its relative volume before and after normalization. This ensured that the total amount of gray matter in each voxel was preserved. Finally, the resulting gray matter images were smoothed with an 8-mm full-width half-maximum (FWHM) isotropic Gaussian kernel.

Voxel-wise comparisons of gray matter volume between groups were performed using two-sample t-tests. Age and gender (Freitas-Ferrari et al., 2010), along with total gray matter volume, were modeled as covariates of no interest. The statistical significance of group differences was set at $p < 0.05$ (combined height threshold $p < 0.005$ and minimum cluster size of 1347 voxels), using the AlphaSim program in the REST toolkit (http://sourceforge.net/projects/resting-fmri). The averaged values of gray matter volume of all voxels in abnormal areas, corrected for age, gender, and total gray matter volume, were correlated with the LSAS (including total score, fear factor, and avoidance factor) using Pearson correlation analysis.

4.4. *Functional connectivity analysis*

The fMRI images (after exclusion of the first five images to ensure steady-state longitudinal magnetization) were initially corrected for temporal differences and head motion. No translation or rotation parameters in any given data set exceeded ±1.5 mm or ±1.5°. Group differences in respect to head translation and rotation have been evaluate elsewhere (Liao et al., 2010a). The functional images were warped into a standard stereotaxic space at a resolution of 3 × 3 × 3 mm^3, using the MNI echo-planar imaging template. At last, the images were spatially smoothed at 8 mm FWHM.

Functional connectivity was investigated using a temporal correlation approach (Fox et al., 2005, 2009). Brain areas showing reduced/increased gray matter volume were defined as seed ROI (the whole significant cluster). To remove possible spurious sources of variance, the time series were preprocessed as follows: first, six head motion parameters, the averaged signals from CSF and white matter, and the global brain signal were regressed (Fox et al., 2005, 2009); next, the time series were band-pass filtered (0.01 ~ 0.08 Hz). A correlation analysis was conducted between the seed ROI and the remaining voxels in the brain. The resulting r values were converted using Fisher's r-to-z transformation to improve the Gaussianity of their distribution.

Individual Z value maps in each group were gathered using one-sample t-test ($p < 0.05$, with false discovery rate [FDR] corrected). To compare the functional connectivity maps between groups, two-sample t-tests were used. Age, gender, and total gray matter volume were also modeled as covariates of no interest. The significance level of group differences was set at $p < 0.05$ (combined height threshold of $p < 0.001$ and a minimum cluster size of 22 voxels). The averaged Z values of all voxels in areas with altered connectivity were corrected for age, gender, and total gray matter volume. Subsequently, they were correlated with the LSAS (including total score, fear factor and avoidance factor) using Pearson correlation analysis.

4.5. *Diffusion tensor imaging tractography analysis*

For DTI, head motion was removed by aligning 15 diffusion-weighted volumes to the unweighted S0 image (b = 0 s/mm^2). Eddy current distortions were corrected by affine registration to the reference S0 image. Whole brain fiber tracking (an interpolated streamline propagation algorithm) was performed in the DTI native space using TrackVis (Schmahmann et al., 2007). Path tracing proceeded until either the fractional anisotropy (FA) was lower than 0.15 or the angle between the current and the previous path segment was higher than 35° (Liao et al., 2010c). As three seed ROI with morphometric alterations were derived from the normalized MNI space, the inverse transformation of the spatial normalization was applied to acquire the seed ROI in the native DTI space (Gong et al., 2009; Liao et al., 2010c). Fiber bundles passing through the three ROI were then extracted from the total collection of brain fibers. For each seed ROI, the connection density (number of connections per unit surface) of fibers can be expressed as $w(e) = \frac{1}{S}\sum_{f \in F_e}\frac{1}{l(f)}$, where, S stands for two-dimensionally intersected surfaces between the individual's white matter and ROI, F_e is a set including all fibers passing through the ROI, and $l(f)$ is the length of fiber f along its trajectory. S corrects for the slightly variable size of intersected surfaces (Hagmann et al., 2008). Mean FA values on the same tract were also extracted. Structural connectivity in three ROI was compared between groups using two-sample t-tests. Age and gender were modeled as covariates of no interest. The significance of group differences in each ROI was set at $p < 0.05$, with Bonferroni correction. Furthermore, the fiber density and mean FA for the three ROI, after correction for age and gender, were correlated with the LSAS (including total score, fear factor, and avoidance factor) using Pearson correlation analysis.

Supplementary materials related to this article can be found online at doi:10.1016/j.brainres.2011.03.018.

Acknowledgments

This research was supported by the Natural Science Foundation of China (Grant nos. 61035006, 90820006 and 30625024 to HC and GQ), the 863 Program (Grant no. 2008AA02Z408 to HC and GQ), the 973 Project (Grant no. 2008CB517407 to WZ), the Flanders Research Foundation (Grant no. A4/5-SDS15387 to DM) and JASC (1A) and JECH (2) are recipients of a CNPq (Brazil) Research Award.

REFERENCES

Amir, N., Klumpp, H., Elias, J., Bedwell, J.S., Yanasak, N., Miller, L.S., 2005. Increased activation of the anterior cingulate cortex during processing of disgust faces in individuals with social phobia. Biol. Psychiatry 57, 975–981.

Arrais, K.C., Machado-de-Sousa, J.P., Trzesniak, C., Santos Filho, A., Ferrari, M.C., Osorio, F.L., Loureiro, S.R., Nardi, A.E., Hetem, L.A., Zuardi, A.W., Hallak, J.E., Crippa, J.A., 2010. Social anxiety disorder women easily recognize fearfull, sad and happy faces: the influence of gender. J. Psychiatr. Res. 44, 535–540.

Ashburner, J., 2007. A fast diffeomorphic image registration algorithm. Neuroimage 38, 95–113.

Ashburner, J., 2009. Computational anatomy with the SPM software. Magn. Reson. Imaging 27, 1163–1174.

Ashburner, J., Friston, K.J., 2005. Unified segmentation. Neuroimage 26, 839–851.

Atmaca, M., Yildirim, H., Ozdemir, H., Ozler, S., Kara, B., Ozler, Z., Kanmaz, E., Mermi, O., Tezcan, E., 2008. Hippocampus and amygdalar volumes in patients with refractory obsessive-compulsive disorder. Prog. Neuropsychopharmacol. Biol. Psychiatry 32, 1283–1286.

Baddeley, R., Abbott, L.F., Booth, M.C., Sengpiel, F., Freeman, T., Wakeman, E.A., Rolls, E.T., 1997. Responses of neurons in primary and inferior temporal visual cortices to natural scenes. Proc. Biol. Sci. 264, 1775–1783.

Birbaumer, N., Grodd, W., Diedrich, O., Klose, U., Erb, M., Lotze, M., Schneider, F., Weiss, U., Flor, H., 1998. fMRI reveals amygdala activation to human faces in social phobics. Neuroreport 9, 1223–1226.

Bishop, S.J., 2007. Neurocognitive mechanisms of anxiety: an integrative account. Trends Cogn. Sci. 11, 307–316.

Blair, R.J., Morris, J.S., Frith, C.D., Perrett, D.I., Dolan, R.J., 1999. Dissociable neural responses to facial expressions of sadness and anger. Brain 122 (Pt 5), 883–893.

Blair, K., Geraci, M., Devido, J., McCaffrey, D., Chen, G., Vythilingam, M., Ng, P., Hollon, N., Jones, M., Blair, R.J., Pine, D.S., 2008a. Neural response to self- and other referential praise and criticism in generalized social phobia. Arch. Gen. Psychiatry 65, 1176–1184.

Blair, K., Shaywitz, J., Smith, B.W., Rhodes, R., Geraci, M., Jones, M., McCaffrey, D., Vythilingam, M., Finger, E., Mondillo, K., Jacobs, M., Charney, D.S., Blair, R.J., Drevets, W.C., Pine, D.S., 2008b. Response to emotional expressions in generalized social phobia and generalized anxiety disorder: evidence for separate disorders. Am. J. Psychiatry 165, 1193–1202.

Boes, A.D., McCormick, L.M., Coryell, W.H., Nopoulos, P., 2008. Rostral anterior cingulate cortex volume correlates with depressed mood in normal healthy children. Biol. Psychiatry 63, 391–397.

Buckner, R.L., Andrews-Hanna, J.R., Schacter, D.L., 2008. The brain's default network: anatomy, function, and relevance to disease. Ann. NY Acad. Sci. 1124, 1–38.

Campbell, D.W., Sareen, J., Paulus, M.P., Goldin, P.R., Stein, M.B., Reiss, J.P., 2007. Time-varying amygdala response to emotional faces in generalized social phobia. Biol. Psychiatry 62, 455–463.

Catani, M., Howard, R.J., Pajevic, S., Jones, D.K., 2002. Virtual in vivo interactive dissection of white matter fasciculi in the human brain. Neuroimage 17, 77–94.

Clark, D.M., Wells, A., 1995. A cognitive model of social phobia. In: Heimberg, R.G., Liebowitz, M.R., Hope, D., Schneider, F. (Eds.), Social phobia: Diagnosis, assessment and treatment. Guildford, New York, pp. 69–93.

Cole, D.M., Smith, S.M., Beckmann, C.F., 2010. Advances and pitfalls in the analysis and interpretation of resting-state FMRI data. Front Syst. Neurosci. 4, 8.

Corbetta, M., Shulman, G.L., 2002. Control of goal-directed and stimulus-driven attention in the brain. Nat. Rev. Neurosci. 3, 201–215.

Critchley, H., 2003. Emotion and its disorders. Br. Med. Bull. 65, 35–47.

Danti, S., Ricciardi, E., Gentili, C., Gobbini, M.I., Pietrini, P., Guazzelli, M., 2010. Is social phobia a "Mis-Communication" disorder? Brain functional connectivity during face perception differs between patients with social phobia and healthy control subjects. Front Syst. Neurosci. 4, 152.

Duncan, J., Owen, A.M., 2000. Common regions of the human frontal lobe recruited by diverse cognitive demands. Trends Neurosci. 23, 475–483.

Etkin, A., Wager, T.D., 2007. Functional neuroimaging of anxiety: a meta-analysis of emotional processing in PTSD, social anxiety disorder, and specific phobia. Am. J. Psychiatry 164, 1476–1488.

Etkin, A., Egner, T., Peraza, D.M., Kandel, E.R., Hirsch, J., 2006. Resolving emotional conflict: a role for the rostral anterior cingulate cortex in modulating activity in the amygdala. Neuron 51, 871–882.

Etkin, A., Keller, K.E., Schatzberg, A.F., Menon, V., Greicius, M.D., 2009. Disrupted amygdalar subregion functional connectivity and evidence for a compensatory network in generalized anxiety disorder. Arch. Gen. Psychiatry 66, 1361–1372.

Ferrari, M.C., Busatto, G.F., McGuire, P.K., Crippa, J.A., 2008. Structural magnetic resonance imaging in anxiety disorders: an update of research findings. Rev. Bras. Psiquiatr. 30, 251–264.

Filho, A.S., Hetem, L.A., Ferrari, M.C., Trzesniak, C., Martin-Santos, R., Borduqui, T., de Lima Osorio, F., Loureiro, S.R., Busatto Filho, G., Zuardi, A.W., Crippa, J.A., 2010. Social anxiety disorder: what are we losing with the current diagnostic criteria? Acta Psychiatr. Scand. 121, 216–226.

Fox, M.D., Snyder, A.Z., Vincent, J.L., Corbetta, M., Van Essen, D.C., Raichle, M.E., 2005. The human brain is intrinsically organized into dynamic, anticorrelated functional networks. Proc. Natl Acad. Sci. U.S.A. 102, 9673–9678.

Fox, M.D., Zhang, D., Snyder, A.Z., Raichle, M.E., 2009. The global signal and observed anticorrelated resting state brain networks. J. Neurophysiol. 101, 3270–3283.

Freitas-Ferrari, M.C., Hallak, J.E., Trzesniak, C., Filho, A.S., Machado-de-Sousa, J.P., Chagas, M.H., Nardi, A.E., Crippa, J.A., 2010. Neuroimaging in social anxiety disorder: a systematic review of the literature. Prog. Neuropsychopharmacol. Biol. Psychiatry 34, 565–580.

Furmark, T., Appel, L., Michelgard, A., Wahlstedt, K., Ahs, F., Zancan, S., Jacobsson, E., Flyckt, K., Grohp, M., Bergstrom, M., Pich, E.M., Nilsson, L.G., Bani, M., Langstrom, B., Fredrikson, M., 2005. Cerebral blood flow changes after treatment of social phobia with the neurokinin-1 antagonist GR205171, citalopram, or placebo. Biol. Psychiatry 58, 132–142.

Gentili, C., Gobbini, M.I., Ricciardi, E., Vanello, N., Pietrini, P., Haxby, J.V., Guazzelli, M., 2008. Differential modulation of neural activity throughout the distributed neural system for

face perception in patients with Social Phobia and healthy subjects. Brain Res. Bull. 77, 286–292.
Goldin, P.R., Manber-Ball, T., Werner, K., Heimberg, R., Gross, J.J., 2009a. Neural mechanisms of cognitive reappraisal of negative self-beliefs in social anxiety disorder. Biol. Psychiatry 66, 1091–1099.
Goldin, P.R., Manber, T., Hakimi, S., Canli, T., Gross, J.J., 2009b. Neural bases of social anxiety disorder: emotional reactivity and cognitive regulation during social and physical threat. Arch. Gen. Psychiatry 66, 170–180.
Gong, G., He, Y., Concha, L., Lebel, C., Gross, D.W., Evans, A.C., Beaulieu, C., 2009. Mapping anatomical connectivity patterns of human cerebral cortex using in vivo diffusion tensor imaging tractography. Cereb. Cortex 19, 524–536.
Hagmann, P., Cammoun, L., Gigandet, X., Meuli, R., Honey, C.J., Wedeen, V.J., Sporns, O., 2008. Mapping the structural core of human cerebral cortex. PLoS Biol. 6, e159.
Honey, C.J., Sporns, O., Cammoun, L., Gigandet, X., Thiran, J.P., Meuli, R., Hagmann, P., 2009. Predicting human resting-state functional connectivity from structural connectivity. Proc. Natl Acad. Sci. U.S.A. 106, 2035–2040.
Iidaka, T., Omori, M., Murata, T., Kosaka, H., Yonekura, Y., Okada, T., Sadato, N., 2001. Neural interaction of the amygdala with the prefrontal and temporal cortices in the processing of facial expressions as revealed by fMRI. J. Cogn. Neurosci. 13, 1035–1047.
Irle, E., Ruhleder, M., Lange, C., Seidler-Brandler, U., Salzer, S., Dechent, P., Weniger, G., Leibing, E., Leichsenring, F., 2010. Reduced amygdalar and hippocampal size in adults with generalized social phobia. J. Psychiatry Neurosci. 35, 126–131.
Ishai, A., Ungerleider, L.G., Martin, A., Schouten, J.L., Haxby, J.V., 1999. Distributed representation of objects in the human ventral visual pathway. Proc. Natl Acad. Sci. U.S.A. 96, 9379–9384.
Johansen-Berg, H., Rushworth, M.F., 2009. Using diffusion imaging to study human connectional anatomy. Annu. Rev. Neurosci. 32, 75–94.
Kahn, I., Andrews-Hanna, J.R., Vincent, J.L., Snyder, A.Z., Buckner, R.L., 2008. Distinct cortical anatomy linked to subregions of the medial temporal lobe revealed by intrinsic functional connectivity. J. Neurophysiol. 100, 129–139.
Kerns, J.G., Cohen, J.D., MacDonald III, A.W., Cho, R.Y., Stenger, V.A., Carter, C.S., 2004. Anterior cingulate conflict monitoring and adjustments in control. Science 303, 1023–1026.
Kilts, C.D., Kelsey, J.E., Knight, B., Ely, T.D., Bowman, F.D., Gross, R.E., Selvig, A., Gordon, A., Newport, D.J., Nemeroff, C.B., 2006. The neural correlates of social anxiety disorder and response to pharmacotherapy. Neuropsychopharmacology 31, 2243–2253.
Koechlin, E., Summerfield, C., 2007. An information theoretical approach to prefrontal executive function. Trends Cogn. Sci. 11, 229–235.
Liao, W., Chen, H., Feng, Y., Mantini, D., Gentili, C., Pan, Z., Ding, J., Duan, X., Qiu, C., Lui, S., Gong, Q., Zhang, W., 2010a. Selective aberrant functional connectivity of resting state networks in social anxiety disorder. Neuroimage 52, 1549–1558.
Liao, W., Qiu, C., Gentili, C., Walter, M., Pan, Z., Ding, J., Zhang, W., Gong, Q., Chen, H., 2010b. Altered effective connectivity network of the amygdala in social anxiety disorder: a resting-state FMRI study. PLoS ONE 5, e15238.
Liao, W., Zhang, Z., Pan, Z., Mantini, D., Ding, J., Duan, X., Luo, C., Wang, Z., Tan, Q., Lu, G., Chen, H., 2010c. Default mode network abnormalities in mesial temporal lobe epilepsy: A Study combining fMRI and DTI. Hum. Brain Mapp., doi:10.1002/hbm.21076.
Lorberbaum, J.P., Kose, S., Johnson, M.R., Arana, G.W., Sullivan, L.K., Hamner, M.B., Ballenger, J.C., Lydiard, R.B., Brodrick, P.S., Bohning, D.E., George, M.S., 2004. Neural correlates of speech anticipatory anxiety in generalized social phobia. Neuroreport 15, 2701–2705.
Machado-de-Sousa, J.P., Arrais, K.C., Alves, N.T., Chagas, M.H., de Meneses-Gaya, C., Crippa, J.A., Hallak, J.E., 2010. Facial affect processing in social anxiety: tasks and stimuli. J. Neurosci. Methods 193, 1–6.
Massana, G., Serra-Grabulosa, J.M., Salgado-Pineda, P., Gasto, C., Junque, C., Massana, J., Mercader, J.M., 2003. Parahippocampal gray matter density in panic disorder: a voxel-based morphometric study. Am. J. Psychiatry 160, 566–568.
Mathew, S.J., Coplan, J.D., Gorman, J.M., 2001. Neurobiological mechanisms of social anxiety disorder. Am. J. Psychiatry 158, 1558–1567.
Miller, E.K., Cohen, J.D., 2001. An integrative theory of prefrontal cortex function. Annu. Rev. Neurosci. 24, 167–202.
Ochsner, K.N., Gross, J.J., 2005. The cognitive control of emotion. Trends Cogn. Sci. 9, 242–249.
Phan, K.L., Liberzon, I., Welsh, R.C., Britton, J.C., Taylor, S.F., 2003. Habituation of rostral anterior cingulate cortex to repeated emotionally salient pictures. Neuropsychopharmacology 28, 1344–1350.
Phan, K.L., Fitzgerald, D.A., Nathan, P.J., Tancer, M.E., 2006. Association between amygdala hyperactivity to harsh faces and severity of social anxiety in generalized social phobia. Biol. Psychiatry 59, 424–429.
Phan, K.L., Orlichenko, A., Boyd, E., Angstadt, M., Coccaro, E.F., Liberzon, I., Arfanakis, K., 2009. Preliminary evidence of white matter abnormality in the uncinate fasciculus in generalized social anxiety disorder. Biol. Psychiatry 66, 691–694.
Potts, N.L., Davidson, J.R., Krishnan, K.R., Doraiswamy, P.M., 1994. Magnetic resonance imaging in social phobia. Psychiatry Res. 52, 35–42.
Raichle, M.E., MacLeod, A.M., Snyder, A.Z., Powers, W.J., Gusnard, D.A., Shulman, G.L., 2001. A default mode of brain function. Proc. Natl Acad. Sci. U.S.A. 98, 676–682.
Schmahmann, J.D., Pandya, D.N., Wang, R., Dai, G., D'Arceuil, H.E., de Crespigny, A.J., Wedeen, V.J., 2007. Association fibre pathways of the brain: parallel observations from diffusion spectrum imaging and autoradiography. Brain 130, 630–653.
Schneider, F., Weiss, U., Kessler, C., Muller-Gartner, H.W., Posse, S., Salloum, J.B., Grodd, W., Himmelmann, F., Gaebel, W., Birbaumer, N., 1999. Subcortical correlates of differential classical conditioning of aversive emotional reactions in social phobia. Biol. Psychiatry 45, 863–871.
Seeley, W.W., Menon, V., Schatzberg, A.F., Keller, J., Glover, G.H., Kenna, H., Reiss, A.L., Greicius, M.D., 2007. Dissociable intrinsic connectivity networks for salience processing and executive control. J. Neurosci. 27, 2349–2356.
Shin, L.M., Liberzon, I., 2010. The neurocircuitry of fear, stress, and anxiety disorders. Neuropsychopharmacology 35, 169–191.
Smith, K.A., Morris, J.S., Friston, K.J., Cowen, P.J., Dolan, R.J., 1999. Brain mechanisms associated with depressive relapse and associated cognitive impairment following acute tryptophan depletion. Br. J. Psychiatry 174, 525–529.
Stein, M.B., Stein, D.J., 2008. Social anxiety disorder. Lancet 371, 1115–1125.
Stein, M.B., Goldin, P.R., Sareen, J., Zorrilla, L.T., Brown, G.G., 2002. Increased amygdala activation to angry and contemptuous faces in generalized social phobia. Arch. Gen. Psychiatry 59, 1027–1034.
Straube, T., Kolassa, I.T., Glauer, M., Mentzel, H.J., Miltner, W.H., 2004. Effect of task conditions on brain responses to threatening faces in social phobics: an event-related functional magnetic resonance imaging study. Biol. Psychiatry 56, 921–930.
Supekar, K., Uddin, L.Q., Prater, K., Amin, H., Greicius, M.D., Menon, V., 2010. Development of functional and structural connectivity within the default mode network in young children. Neuroimage 52, 290–301.
Tillfors, M., Furmark, T., Marteinsdottir, I., Fischer, H., Pissiota, A., Langstrom, B., Fredrikson, M., 2001. Cerebral blood flow in

subjects with social phobia during stressful speaking tasks: a PET study. Am. J. Psychiatry 158, 1220–1226.
Tillfors, M., Furmark, T., Marteinsdottir, I., Fredrikson, M., 2002. Cerebral blood flow during anticipation of public speaking in social phobia: a PET study. Biol. Psychiatry 52, 1113–1119.
Vincent, J.L., Kahn, I., Snyder, A.Z., Raichle, M.E., Buckner, R.L., 2008. Evidence for a frontoparietal control system revealed by intrinsic functional connectivity. J. Neurophysiol. 100, 3328–3342.
Warwick, J.M., Carey, P., Jordaan, G.P., Dupont, P., Stein, D.J., 2008. Resting brain perfusion in social anxiety disorder: a voxel-wise whole brain comparison with healthy control subjects. Prog. Neuropsychopharmacol. Biol. Psychiatry 32, 1251–1256.
Wignall, E.L., Dickson, J.M., Vaughan, P., Farrow, T.F., Wilkinson, I.D., Hunter, M.D., Woodruff, P.W., 2004. Smaller hippocampal volume in patients with recent-onset posttraumatic stress disorder. Biol. Psychiatry 56, 832–836.
Zhao, X.H., Wang, P.J., Li, C.B., Hu, Z.H., Xi, Q., Wu, W.Y., Tang, X.W., 2007. Altered default mode network activity in patient with anxiety disorders: an fMRI study. Eur. J. Radiol. 63, 373–378.